Current-driven vortex domain wall dynamics by micromagnetic simulations

J. He, Z. Li, and S. Zhang

Department of Physics and Astronomy, University of Missouri–Columbia, Columbia, Missouri 65211, USA

Current-driven vortex wall dynamics is studied by means of a two-dimensional analytical model and micromagnetic simulation. By constructing a trial function for the vortex wall in the magnetic wire, we analytically solve for domain wall velocity and deformation in the presence of the current-induced spin torque. A critical current for the domain wall transformation from the vortex wall to the transverse wall is calculated. A comparison between the field- and current-driven wall dynamics is carried out. Micromagnetic simulations are performed to verify our analytical results.

I. INTRODUCTION

Magnetic domain walls in magnetic films have various structural forms which are determined by geometrical and material parameters. For a magnetic wire with an "infinite" length and a finite width, there are commonly two types of domain walls: transverse walls (TWs) and vortex walls (VWs). Both of them are stable. Depending on the wire thickness and width, one of the walls is usually more stable.[1,2] However, in a certain range of the parameters, the static energies of these two walls are comparable and thus one can produce both types of walls in the same wire. By using different initialization methods, one can create either wall.[1] When a magnetic field or an electric current is applied, both TWs and VWs are able to move along the wire. The dynamics of the walls is generally very complex and micromagnetic simulations are required in order to describe the details of the domain wall motion. For the TW, a simplified and yet very insightful analytical treatment was developed by Walker.[3] A one-dimensional (1D) wall profile, i.e., the magnetization direction in the wall depends only on the coordinate along the wire, has been used to approximate the TW profile. With this approach, one can analytically calculate the wall velocity and wall distortion in the presence of magnetic field and electrical current.[4] For the VW, however, the 1D wall profile fails to capture the wall structure and one needs at least to use a 2D model to approximately characterize the vortex structure. In this paper, we propose such a 2D model for the VW. Our focus will be on the analytical calculation of the dynamic behavior of the VW. Within our model, we are able to describe the vortex wall motion, including the wall distortion, wall velocity, and wall structure transformation, in terms of material parameters and external magnetic field or electric current. In particularly, we show how the vortex core moves toward the edge of the wire when a current or a field is applied along the wire. With a sufficiently large current or field, the vortex core may vanish at the boundaries of the wire edges and the transformation from the VW to the TW occurs. This paper is organized as follows. In Sec. II, we develop the analytical 2D model for the VW. An equation of motion for the domain wall is established. The steady state motions driven by the current and by the field are investigated. We also compare the dynamics between the TW and the VW. In Sec. III, the micromagnetic

simulations are performed. We compare the simulated results with the analytical ones. Finally, we summarize the different features of dynamics for TWs and VWs in Sec. IV.

II. ANALYTICAL MODEL

A. Equation of motion

We start with the generalized Landau-Lifshitz-Gilbert equation including the spin-transfer torque terms:[5]

$$\frac{\partial \mathbf{M}}{\partial t} = -\gamma \mathbf{M} \times \mathbf{H}_{eff} + \frac{\alpha}{M_s} \mathbf{M} \times \frac{\partial \mathbf{M}}{\partial t} - \frac{b_J}{M_s^2} \mathbf{M} \times \left(\mathbf{M} \times \frac{\partial \mathbf{M}}{\partial x} \right)$$

$$- \frac{c_J}{M_s} \mathbf{M} \times \frac{\partial \mathbf{M}}{\partial x} \quad (1)$$

where γ is the gyromagnetic ratio, $\mathbf{H}_{eff} = -\frac{\delta W}{\delta \mathbf{M}}$ is the effective magnetic field, and W is the total energy density which could be written as $W = A(\nabla \mathbf{m})^2 + (K/M_s^2)(\mathbf{M} \times \mathbf{e}_x)^2 - \mathbf{H}_e \cdot \mathbf{M} - (1/2)\mathbf{H}_d \cdot \mathbf{M}$, where A is the exchange constant, K is the anisotropy, $\mathbf{H}_e$ is the external field, and $\mathbf{H}_d$ is the magnetostatic field. α is the Gilbert damping parameter, and $b_J = Pj_e\mu_B/eM_s(1+\xi^2)$ and $c_J = \xi b_J$, where P is the spin polarization of the current; j_e is the current density along the length direction of the magnetic wire; μ_B is the Bohr magneton, M_s is the saturation magnetization, and ξ (small, $\sim \alpha$) is a dimensionless constant which describes the degree of the nonadiabaticity between the spin of the nonequilibrium conduction electrons and the local magnetization.

To describe the motion of an entire domain wall, it is useful to introduce a total force acting on the wall. Following Thiele,[6] we define the total force

$$\mathbf{F}\{\theta, \phi\} \equiv \int dV \, \boldsymbol{\nabla} W = \int \left(\frac{\delta W}{\delta \theta}(\boldsymbol{\nabla}\theta) + \frac{\delta W}{\delta \phi}(\boldsymbol{\nabla}\phi) \right) dV \quad (2)$$

where θ and ϕ are the angular components of $\mathbf{M}$ in the spherical coordinate. For the steady-state motion of a domain wall, we may write $\theta = \theta(\mathbf{r} - \mathbf{v}t)$, $\phi = \phi(\mathbf{r} - \mathbf{v}t)$, where $\mathbf{v}$ is the steady velocity, then we have

$$\dot{\theta} = -\mathbf{v} \cdot \boldsymbol{\nabla}\theta, \quad \dot{\phi} = -\mathbf{v} \cdot \boldsymbol{\nabla}\phi. \quad (3)$$

The above steady-state condition immediately reduces the temporal-spatial differential equation, Eq. (1), to a differen-

tial equation with spatial variables only. By writing Eq. (1) in the angular components and by placing them into Eq. (2), we obtain the equation of motion for the domain wall[7]

$$\mathbf{F} + \mathbf{G} \times (\mathbf{v} + b_J\hat{\mathbf{x}}) + \mathcal{D} \cdot (\alpha\mathbf{v} + c_J\hat{\mathbf{x}}) = 0 \qquad (4)$$

where $\mathbf{G}$ is the domain gyrocoupling vector

$$\mathbf{G} = -M_s\gamma^{-1} \int dV \sin\theta(\boldsymbol{\nabla}\theta \times \boldsymbol{\nabla}\phi) \qquad (5)$$

and $\mathcal{D}$ is the domain dissipation dyadic (tensor)

$$\mathcal{D} = -M_s\gamma^{-1} \int dV(\boldsymbol{\nabla}\theta\,\boldsymbol{\nabla}\theta + \sin^2\theta\,\boldsymbol{\nabla}\phi\,\boldsymbol{\nabla}\phi). \qquad (6)$$

The domain wall force defined in Eq. (2) can be simplified when the domain wall undergoes uniform motion. Let us separate the force in terms of the internal force $\mathbf{F}^{in}$ and the external force $\mathbf{F}^{ext}$,

$$\mathbf{F} = \mathbf{F}^{in} + \mathbf{F}^{ext}. \qquad (7)$$

$\mathbf{F}^{in}$ contains all the forces from the internal energy including anisotropy energy, exchange energy, and magnetostatic energy. When one sums over the internal energy contribution, the total internal force vanishes due to Newton's third law. Therefore, one may simply consider the external energy contribution to the force in Eqs. (4) and (2), i.e.,

$$\mathbf{F} = \mathbf{F}^{ext} = \int dV\left((\boldsymbol{\nabla}\theta)\frac{\partial}{\partial\theta} + (\boldsymbol{\nabla}\phi)\frac{\partial}{\partial\phi}\right)(-\mathbf{H}\cdot\mathbf{M}), \qquad (8)$$

where we have assumed that the external energy is solely from the external field, $W = -\mathbf{H}\cdot\mathbf{M}$. We will show later that we must consider other external forces on the vortex wall when the wall reaches the boundary of the wire. Note that if the profile of domain structures [i.e., $\mathbf{M}(\mathbf{x},\mathbf{y},\mathbf{z})$ in the moving frame of the steady motion] is determined, the gyrocoupling vector, dissipation dyadic, and static force can be calculated from Eqs. (5), (6), and (8), and the steady velocity will be then readily derived from Eq. (4).

In this section, we shall apply the equation of motion, Eq. (4), to study the domain wall velocity of the vortex wall, driven by an external magnetic field and by spin-transfer torques. Let us first consider a simplified head-to-head transverse wall as shown in Fig. 1(a). For the transverse wall, we assume the wall profile can be modeled by the Walker trial function,[3]

$$\phi(x) = 2\tan^{-1}\exp\left(\frac{x}{\Delta}\right), \quad \theta(x) = \frac{\pi}{2}, \qquad (9)$$

where $\phi(x)$ and $\theta(x)$ are the angles between the direction of the magnetization and the wire length direction (+x axis) and wire plane normal (+z axis), respectively. Δ is the domain wall width. By placing the above wall profile into Eqs. (5)–(8), we find that the gyrocoupling vector is zero, $\mathbf{G} = \mathbf{0}$, and the dissipation dyadic has only one nonzero component $\mathcal{D}_{xx} = -2M_s/\gamma\Delta$. The external force is $\mathbf{F} = 2HM_s\hat{\mathbf{x}}$. By inserting them into Eq. (4), we immediately find the velocity:
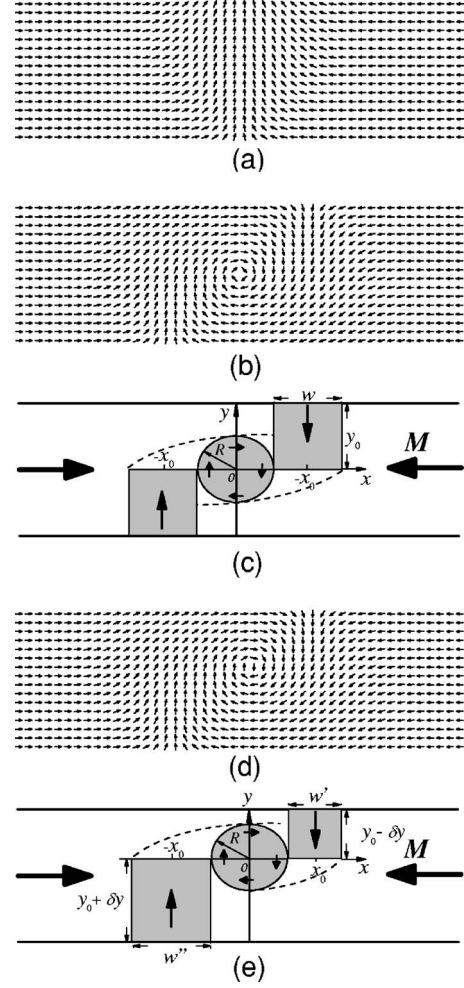

FIG. 1. Magnetization patterns of (a) a transverse wall and (b) a vortex wall, without an applied current or field. (c) Schematic model for the vortex wall (b): a vortex wall is modeled by two TWs and a vortex core, shown in gray areas. The vortex core is at the center of the wire and $\pm x_0$ are the positions of the centers of the TWs. R is the outer radius of the vortex core, w is the wall width of two TW walls, and y_0 is the half-width of the wire. (d) The magnetization pattern of the vortex wall in the presence of the current, which is calculated by micromagnetic simulation in Sec. III. The parameters are the spin torque $b_J = 25$ m/s, damping parameter $\alpha = 0.05$, and nonadiabaticity coefficient $\xi = 0.04$. (e) The schematic model for the vortex wall (d). δy is the displacement of the vortex toward the edge of the wire. The wall structure is not symmetrical, and one TW is expanded and the other is compressed.

$$v_x = \frac{\gamma H\Delta}{\alpha} - \frac{c_J}{\alpha}. \qquad (10)$$

This result had been obtained previously.[3,4,7]

It is difficult to analytically model the profile of the vortex wall depicted in Fig. 1(b) by a single elementary function as we did for the transverse wall. From previous simulation results,[1,2] the VW structure might be understood as two symmetrical transverse walls diagonally crossing the wire and a central vortex core connecting the two TWs. It is noted that the two TWs have opposite polarities, namely, the magneti-

zations of the centers of these two TWs orient in opposite directions. The transitional region between these two TWs is sometimes called the Bloch line,[8] which characterizes the wall-polarity reversal in analogy to the Bloch wall. For the VW we consider here, this transitional region contains a vortex core. The magnetization of the inner vortex core has a significant out-of-plane component and thus the inner radius of the vortex core must be very small since the out-of-plane magnetization enhances demagnetization energy.[9] Outside the inner vortex core the magnetization lies in the plane and the outer radius of the vortex core is limited by the transverse wall width and the wire width. To characterize the entire VW profile, we separate the wall into *three* parts: two transverse walls and a vortex core [schematically shown in Figs. 1(c) and 1(e)], and for the model in Fig. 1(e), they will be assigned to different trial functions given below. For the vortex part,[9–12]

$$
\theta =
\begin{cases}
2\tan^{-1}\left(\dfrac{\sqrt{x^2+y^2}}{r_{core}}\right) & (0 \leqslant x^2+y^2 < r_{core}^2), \\[3mm]
\dfrac{\pi}{2} & (r_{core}^2 \leqslant x^2+y^2 < R^2),
\end{cases}
$$

$$
\phi = q \arg(x+iy) + c\frac{\pi}{2} \quad (0 \leqslant x^2+y^2 \leqslant R^2), \quad (11)
$$

where r_{core} and R are the inner-core and outer radius of the vortex, respectively, q ($=\pm 1, \pm 2, \dots$) is the vorticity of the vortex, c ($=\pm 1$) is the chirality of the vortex, and $i=\sqrt{-1}$. Here we just use the arg function of the complex variable $x+iy$ as a convenient way to express ϕ.[11] In this paper, we consider only a single vortex ($q=1$). And we note that the vortex profile we introduced in Eq. (11) does not include its image profile.[11] For the wire structure, the image profile consists of a series of terms formed by multiple reflections of two wire boundary planes. Including these images would make the analytical calculation intractable. Instead, we introduce a "restoring force"[13] due to the induced charges along the boundaries of the nanowire. This restoring force has a similar role to the image vortices in the method of images.[11] For the two transverse walls[3,4] where ($-\infty < x < +\infty$),

$$
\theta = \pi/2 \quad (-y_0 \leqslant y \leqslant y_0),
$$

$$
\phi =
\begin{cases}
2\tan^{-1}\exp\left(\dfrac{x+x_0}{w''}\right) & (-y_0-\delta y \leqslant y \leqslant 0), \\[3mm]
2\tan^{-1}\exp\left(\dfrac{x-x_0}{w'}\right) & (0 \leqslant y \leqslant y_0-\delta y),
\end{cases}
$$

$$
(12)
$$

where x_0 is the distance from the center of each TW part to the vortex core center, w' and w'' are the wall widths of two TWs, y_0 is the half-width of the magnetic wire, and δy is the displacement of the vortex core away from the wire center in the y direction. We realize that the TW and vortex core defined above are not strictly valid because the TW is extended to the vortex region when $0 \leqslant x^2+y^2 \leqslant R^2$. However, this ill-

defined overlapped region does not contribute significant errors since $\nabla\theta$ and $\nabla\phi$ are exponentially small in this region. By using the above wall profile, we are able to calculate $\mathbf{G}$, $\mathcal{D}$, and $\mathbf{F}$ defined in Eqs. (5), (6), and (8) in a similar way as the calculations in Refs. 14 and 15. The steady-state velocity can then be calculated from Eq. (4).

1. Current-driven domain wall motion

We consider the current-driven vortex wall motion without the external field so that $\mathbf{F}=\mathbf{0}$ [see Eq. (8)]. Let us apply the equation of motion, Eq. (4), to the vortex part of the wall and neglect its interaction with two TW parts. By placing Eq. (11) into Eqs. (5) and (6), we find the explicit expressions for $\mathbf{G}$ and $\mathcal{D}$:

$$
\mathbf{G} = -2\pi M_s \gamma^{-1} p\hat{\mathbf{z}} = G_v\hat{\mathbf{z}}, \quad (13)
$$

$$
\mathcal{D} = -M_s \gamma^{-1}\pi \ln\frac{R}{a}(\hat{\mathbf{x}}\hat{\mathbf{x}}+\hat{\mathbf{y}}\hat{\mathbf{y}}) = \mathcal{D}_v(\hat{\mathbf{x}}\hat{\mathbf{x}}+\hat{\mathbf{y}}\hat{\mathbf{y}}) \quad (14)
$$

where $\hat{\mathbf{x}},\hat{\mathbf{y}},\hat{\mathbf{z}}$ are unit vectors in the directions of the wire length, width, and thickness, respectively. p ($=\pm 1$) represents the polarity of the vortex core [$\theta(0)=0$ or π], and a is the lattice constant of the crystal structure of the wire material. Note that in the calculation of $\mathcal{D}$, we have neglected a small part of the vortex core ($\sim a^2$), and this does not considerably affect the wall dynamics.[14] By placing Eqs. (13) and (14) and $\mathbf{F}=\mathbf{0}$ into Eq. (4), we have

$$
-G_v v_y + \mathcal{D}_v(\alpha v_x + c_J) = 0,
$$

$$
G_v(v_x + b_J) + \alpha\mathcal{D}_v v_y = 0, \quad (15)
$$

and one immediately finds

$$
v_{x_0} = -b_J\frac{G_v^2+\alpha\xi\mathcal{D}_v^2}{G_v^2+\alpha^2\mathcal{D}_v^2} \cong -b_J \quad (\alpha \ll 1, \xi \ll 1),
$$

$$
v_{y_0} \cong -\frac{1}{2}b_J p(\alpha-\xi)\ln\frac{R}{a}. \quad (16)
$$

It is shown that the velocity of the VW has two components: v_{x_0} along the wire and v_{y_0} perpendicular to the wire. The nonzero v_{y_0} (except for $\xi=\alpha$) is caused by the gyrotropic term (nonzero G) of the vortex dynamics.[6] The sign of v_{y_0} (to which edge of the wire) is determined by the sign of the product $p(\alpha-\xi)$, i.e., it is vortex polarity (p) dependent. If we characterize the vortex by a Bloch line, the perpendicular motion might be understood in terms of the moving Bloch line inside and along the wall surface.[8]

We recall that the velocity of the TW is $v_x=-c_J/\alpha$ and $v_y=0$ in the steady state motion. The different velocities for the vortex core and the transverse wall cannot be a steady state solution for the entire wall. In fact, the interaction between these different parts of the wall must be included in order to reach a common velocity in the steady state. One can immediately see that the motion of the vortex core along the y direction would push one TW and pull the other. As a result, one TW expands and the other gets compressed [see

Fig. 1(e)]. Conversely, these distorted TWs would produce a reacting force to the vortex core; sometimes it is called a restoring force.[7,10,16] If we model the forces between the vortex core and the TW by elastic potentials in analogy to spring-connected particles, we must add the spring force as an external force when one applies Eq. (4) to each individual part of the vortex wall. Then, two scenarios are possible: the reacting force is strong enough to completely halt the perpendicular wall velocity; or the reacting force is unable to stop the vortex from colliding with the wall edge. In the former case, the perpendicular wall velocity eventually reaches zero and a steady state wall velocity along the wire is achieved. The final wall velocity is precisely the same as that of the transverse wall (i.e., $v_x = -c_J/\alpha$ and $v_y = 0$; see the calculations below). In the latter case, the vortex core collides with the wire edge and can either vanish (move out of the wire) or be reflected, i.e., the transformation of the vortex wall to other types of walls occurs. Usually, the vortex core disappears at the edge and the wall becomes a TW.[17]

When a steady state motion is achieved, we may apply Eq. (4) to the entire wall. The interaction between the vortex core and the TWs becomes an internal force and does not enter Eq. (4). However, there is an external force acting on the entire wall, which is due to the magnetic charges coming from the distorted TW parts at the boundaries. This force is again analogous to the counteractive force from fixed boundaries to compressed springs. If we model this force as linearly dependent on the displacement of the vortex core δy in the y direction, i.e., $F^{re} = -\kappa \delta y$, where the constant κ is discussed in Ref. 13, we find, from Eq. (4),

$$-G_v v_y + \mathcal{D}_{xx}(\alpha v_x + c_J) = 0,$$

$$-\kappa \delta y + G_v(v_x + b_J) + \alpha \mathcal{D}_{yy} v_y = 0, \qquad (17)$$

where we have used and determined

$$\mathbf{G} = G_v \hat{\mathbf{z}}, \qquad (18)$$

$$\mathcal{D} = (\mathcal{D}_v + \mathcal{D}_t)\hat{\mathbf{x}}\hat{\mathbf{x}} + \mathcal{D}_v \hat{\mathbf{y}}\hat{\mathbf{y}} = \mathcal{D}_{xx}\hat{\mathbf{x}}\hat{\mathbf{x}} + \mathcal{D}_{yy}\hat{\mathbf{y}}\hat{\mathbf{y}} \qquad (19)$$

where $\mathcal{D}_t = -2M_s \gamma^{-1}\left(\frac{y_0 - \delta y}{w'} + \frac{y_0 + \delta y}{w''}\right)$. Note that the TW parts have no contribution to the gyrocoupling vector $\mathbf{G}$; however, they modify the dissipation dyadic with $\mathcal{D}_t$.

In the steady state of motion, $v_y = 0$, we immediately find from Eq. (17)

$$v_x = -\frac{c_J}{\alpha} \qquad (20)$$

and

$$\delta y = \frac{G_v b_J}{\kappa}\left(1 - \frac{\xi}{\alpha}\right). \qquad (21)$$

The above simplified analysis shows that the steady state domain wall velocity is a universal constant $v_x = -c_J/\alpha$, independent of the wall structure, as long as the restoring force from the edges of the wire is strong enough to halt the wall motion in the direction perpendicular to the wire. We can qualitatively estimate the critical current b_J^c when the restor-

ing force just barely prevents the wall colliding with the wire edge, i.e., when $\delta y = y_0$ (y_0 is the half-width of the wire). By using Eq. (21), we have

$$b_J^c = \frac{\kappa y_0}{G_v}\left(1 - \frac{\xi}{\alpha}\right)^{-1}. \qquad (22)$$

If the current is larger than the above current density, the restoring force is unable to stop the vortex core colliding with the boundary and the VW transforms into a TW. The wall transformation may be qualitatively understood in terms of the conservation of the topological charges:[12] when the vortex core reaches the edge, the vortex with the winding number +1 is absorbed by one of the edge defects (one of the transverse wall parts) with winding number −1/2; then a +1/2 edge defect must be created to conserve the topological charges. This +1/2 edge defect together with the −1/2 edge defect on the other side of the wire edge is equivalent to a simple transverse wall with a uniform polarity.

2. Field-driven domain wall motion

By adding the external force due to the magnetic field [defined in Eq. (8)] to Eq. (17), we can similarly derive the domain wall steady motion velocity. In the steady state, the external force on the entire wall is

$$\mathbf{F} = 4y_0 H M_s \hat{\mathbf{x}} + c\pi H M_s(R - a)\hat{\mathbf{y}} = F_x \hat{\mathbf{x}} + F_y \hat{\mathbf{y}}. \qquad (23)$$

In the absence of the current where $c_J = b_J = 0$, we find that from Eq. (17) the steady state velocity along the wire ($v_y = 0$) is

$$v_x = -\frac{F_x}{\alpha \mathcal{D}_{xx}} = \frac{\gamma H y_0}{\alpha}\left(\frac{4}{\pi \ln \dfrac{R}{a} + 2\left(\dfrac{y_0 - \delta y}{w'} + \dfrac{y_0 + \delta y}{w''}\right)}\right) \tag{24}$$

and the displacement of the vortex center in the direction of the wire width is

$$\delta y = \frac{G_v v_x + F_y}{\kappa}. \qquad (25)$$

As in the case of the TW, the wall velocity is not universal and it depends on the details of the wall structure. Compared with a TW, the velocity of the VW is smaller;[18] this can be qualitatively understood in terms of a smaller wall width for the VW. Let us take the width of the TW part[2] as $\frac{y_0 - \delta y}{w'} = \frac{y_0 + \delta y}{w''} = \pi$ (again, y_0 is the half-width of the wire). And the width of the TW [Δ in Eq. (9)] in the same wire is also taken as $\Delta = 2y_0/\pi$. For the VW, we may define an effective wall width from Eq. (24):

$$w_{vw} = \Delta\left(\frac{1}{2 + \dfrac{1}{2}\ln \dfrac{R}{a}}\right). \qquad (26)$$

For example, for a wire $R = w/2 = 20$ nm and the lattice constant $a = 0.5$ nm, the ratio of the TW to VW velocity is about $2 + \frac{1}{2}\ln \frac{R}{a} = 3.8$.

When the magnetic field is large, the restoring force is unable to stop the wall colliding with the wall edge. The vortex wall will be annihilated and the transformation to the TW occurs. Similarly, we may estimate the critical field H_e^c for the wall transformation by the condition $\delta y = y_0$. We thus find

$$H^c = \kappa y_0 \left(\frac{\gamma G_v w_{vw}}{\alpha} + c \pi M_s (R - a) \right)^{-1}. \qquad (27)$$

III. MICROMAGNETIC SIMULATION

A. Simulation procedure

To verify the analytical results derived above, we perform micromagnetic simulations by directly solving Eq. (1) for a defect-free magnetic wire sample. The geometrical size of the wire is 2 μm long (x direction), 128 nm wide (y direction), and 8 nm thick (z direction). The grid size is taken as $4 \times 4 \times 8$ nm^3. The material parameters are the exchange constant $A = 1.3 \times 10^{-6}$ erg/cm, the anisotropy field $H_K = 0$ (Oe), the saturation magnetization $M_s = 800$ emu/cc, the spin polarization $P = 0.5$, and the damping parameter α and the non-adiabaticity factor ξ varying from 0.01 to 0.08.

The magnetization at both ends is set to be along the x direction and directed inward to the wire and we use free boundary conditions for the other dimensions. Since the domain wall may move several micrometers in some cases, it is important to keep the domain wall far away from the ends to reduce the influence of magnetostatic fields from the wire ends: we shift the x coordinate of the entire domain wall after each numerical iteration so that the center of the wall is always located at the center of the wire. By using two initial domain configurations similar to Ref. 1 we generate two types of walls in the middle of the wire, the TW in Fig. 1(a) and the VW. The VW has four equivalent configurations corresponding to different polarity ($p = \pm 1$) and chirality ($c = \pm 1$). We only show the VW for $p = -1$ and $c = 1$ in Fig. 1(b) The TW and VW shown in Fig. 1 are our initial wall configurations. At time $t = 0$, a constant spin torque or a magnetic field is applied to the wire, and we calculate the wall motion as a function of time until the wall reaches steady motion or until a sufficiently long time that the wall motion remains nonuniform.

B. Simulation results

To compare the analytical results on the universal domain wall velocity, we first consider applying a sufficiently small spin torque ($b_J = 25$ m/s) so that the vortex core remains inside the wire. We vary the damping parameter α and nonadiabaticity coefficient ξ from 0.01 to 0.08 to determine the relation between the domain wall velocity and these two parameters. In Fig. 2 we show that the initial velocity of the VW in the x direction is always b_J (independent of α and ξ), while the total displacement of the center of the wall in the y direction quantitatively agrees with Eq. (21). As expected, the y-component velocity gradually reduces to zero when the center of the core moves toward the edge. The restoring
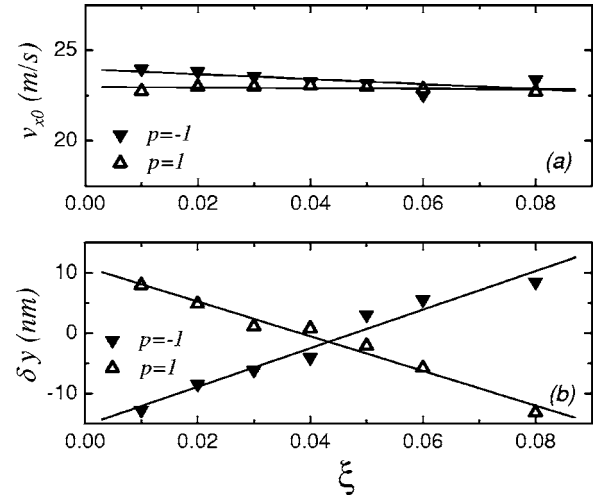

FIG. 2. The dependence of (a) the x component of the initial velocity v_{x_0} and (b) the y-component displacement δy as a function of the nonadiabaticity parameter ξ for two different polarity VWs ($p = \pm 1$). We have used $b_J = 25$ m/s and $\alpha = 0.05$. The straight lines are simple data fits.

force eventually stops the wall motion in the y direction, and a steady state motion with the velocity $v_x = -c_J/\alpha$ along the x direction is reached. In Fig. 3, we show the relations of the terminal velocity v_x with both α and ξ. These simulated results are in excellent agreement with our analytical formula.

When we increase the applied current density (or the strength of the spin torques) above a critical value, the simulations show that the vortex core moves outside the nanowire from the edge and the VW transforms to a TW. The transformed TW moves at the velocity $-c_J/\alpha$.[19] We note that the critical current density depends on the parameters. A special case is when $\xi = \alpha$. We find that the VW can maintain its wall structure up to a much higher current density. This is because the vortex wall does not move toward the wire edge [see Eq. (21)]. However, this accidental case should not be considered as a general property of the VW motion. When the current density is further increased, the TW will also deform during
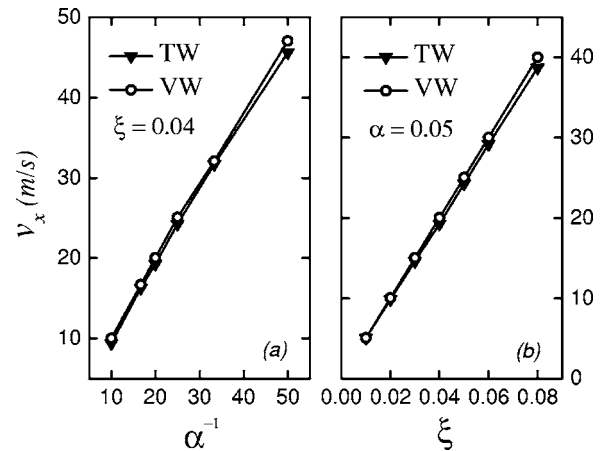

FIG. 3. Steady state velocity of TW and VW as a function of (a) the damping parameter, and (b) the nonadiabaticity parameter. The current density is $b_J = 25$ m/s. The straight lines are simple data fits.

its motion and the velocity is highly nonuniform; this is known as Walker's breakdown.[3] The alternative appearance of a transverse wall and a vortex wall (or antivortex wall)[20] is seen in simulations (not shown here). In our analytical calculations, we exclude these extremely complicated wall dynamics.

As a comparison, we also simulate the field-driven domain wall motion at sufficiently small fields. The behavior of the VW driven by a field is similar to the current-driven case: namely, besides the motion along the wire, the vortex core moves toward the edge and eventually stops due to the restoring force. At a critical field, the VW overcomes the restoring force and the VW transforms into a TW. While the steady velocities of TW and VW are both proportional to the magnetic field H and α^{-1} (see Fig. 4), the VW has a smaller velocity compared to the TW for the same field.

Finally, we point out that the analytical and simulation analysis in this paper is for a defect-free wire. In a realistic wire, defects are unavoidable. We expect that our analytical results may not be applicable. For example, the steady state wall velocity may not be universal and the defect pinning depends on the detail of the wall structure. Indeed, we have seen in our earlier simulation[19] that the critical current is larger for depinning a TW than for a VW. An even more remarkable finding is that the VW first begins depinning and then transforms to a TW, which is finally pinned by defects again (the wall stops). The phenomenon occurs when one applies a moderate current density between the critical values of two depinning currents of the VW and TW.[19] The above feature has been captured in a recent experiment.[17]

IV. CONCLUSION

In summary, we have calculated the velocity of the VW in the magnetic wire. In a defect-free wire, the terminal velocity
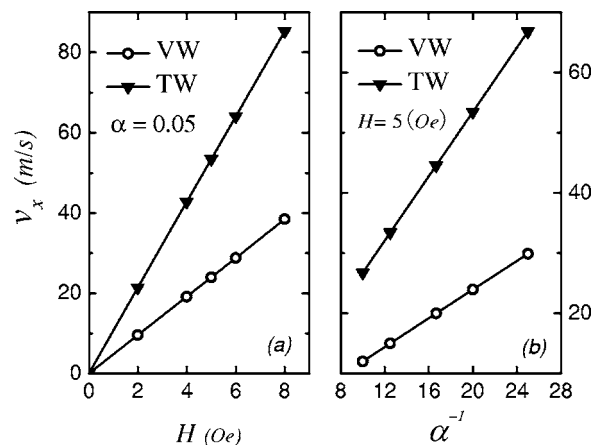

FIG. 4. Steady state velocities of both TW and VW as functions of (a) the magnetic field and (b) the damping parameter. The current density is $b_J = 25$ m/s. The straight lines are simple data fits.

is independent of the wall structure for the current-driven steady motion, while for the field-driven case, the effective domain wall width is a key parameter for the domain wall mobility. The transformation between the VW and the TW is explained as the consequence of the perpendicular motion of the vortex core and the conservation of topological charges. Our model is further supported by numerical solutions and is in agreement with experimental results.

[1] R. D. McMichael and M. J. Donahue, IEEE Trans. Magn. **33**, 4167 (1997).

[2] Y. Nakatani, A. Thiaville, and J. Miltat, J. Magn. Magn. Mater. **290-291**, 750 (2005).

[3] N. L. Schryer and L. R. Walker, J. Appl. Phys. **45**, 5406 (1974).

[4] Z. Li and S. Zhang, Phys. Rev. B **70**, 024417 (2004); Phys. Rev. Lett. **92**, 207203 (2004).

[5] S. Zhang and Z. Li, Phys. Rev. Lett. **93**, 127204 (2004).

[6] A. A. Thiele, Phys. Rev. Lett. **30**, 230 (1973); J. Appl. Phys. **45**, 377 (1974).

[7] A. Thiaville, Y. Nakatani, J. Miltat, and Y. Suzuki, Europhys. Lett. **69**, 990 (2005).

[8] A. P. Malozemoff and J. C. Slonczewski, *Magnetic Domain Walls in Bubble Materials* (Academic Press, New York, 1979).

[9] S. Hikami and T. Tsuneto, Prog. Theor. Phys. **63**, 387 (1980).

[10] K. Y. Guslienko, V. Novosad, Y. Otani, H. Shima, and K. Fukamichi, Appl. Phys. Lett. **78**, 3848 (2001).

[11] J. P. Zagorodny, Y. Gaididei, D. D. Sheka, J. G. Caputo, and F. G. Mertens, Phys. Rev. Lett. **93**, 167201 (2004).

[12] O. Tchernyshyov and G. W. Chern, Phys. Rev. Lett. **95**, 197204 (2005).

[13] While the calculation of the restoring force depends on details of the wall structure, one can estimate it as follows. Consider a simple TW in the wire; the wall energy $E(w) = 2A/w + 2Kw$, where A is the exchange constant, w is the wall width, and K is the anisotropy constant. At equilibrium, the wall width w_0 is determined by $\partial E/\partial w_0 = 0$, i.e., $w_0 = \sqrt{A/K}$. When the wall width is compressed or expanded, the wall energy can be expanded, up to the second order of $w - w_0$, $E(w) = E(w_0) + (2K/w_0)(w - w_0)^2$. Equivalently, the restoring force due to the wall width change is $F = -(4K/w_0)(w - w_0)$. In the present geometry, we approximate the width as $(y_0 - \delta y)/w' = (y_0 + \delta y)/w'' = \pi^2$. We take $\delta y = \pi \delta w$; the restoring force due to the displacement of the vortex core in the y direction is then $F^{re} = -\kappa \delta y$, where $\kappa = 4K/\pi w_0$. When the vortex reaches the boundary, the magnetostatic energy contribution due to the surface charges along the boundary must be included in evaluating κ. A detailed calculation can be found in Ref. 10.

[14] D. L. Huber, Phys. Rev. B **26**, 3758 (1982).

[15] J. C. Slonczewski, J. Magn. Magn. Mater. **12**, 108 (1979).

[16] K. Y. Guslienko, B. A. Ivanov, V. Novosad, Y. Otani, H. Shima, and K. Fukamichi, J. Appl. Phys. **91**, 8037 (2002).

[17] M. Kläui, P.-O. Jubert, R. Allenspach, A. Bischof, J. A. C. Bland, G. Faini, U. Rüdiger, C. A. F. Vaz, L. Vila, and C. Vouille, Phys. Rev. Lett. **95**, 026601 (2005).

[18] A. P. Malozemoff and J. C. Slonczewski, Phys. Rev. Lett. **29**, 952 (1972).

[19] J. He, Z. Li, and S. Zhang, cond-mat/0508736 (unpublished).

[20] Y. Nakatani, A. Thiaville, and J. Miltat, Nat. Mater. **2**, 521 (2003).